www.coast.oaustech.edu.ng
COAST
JOURNAL OF THE SCHOOL OF SCIENCE
Volume 4, Issue 1. May 2022 ISSN: 2714-3716
Coast, J. Sch. Sci. 4 (1): 768 - 781

PREDICTING GEOMAGNETIC STORMS FROM SOLAR WIND PARAMETERS

Bakare, N.O.

Department of Physical Science, Olusegun Agagu University of Science & Technology, Okitipupa, Nigeria
Corresponding Author's Email: sesanbakare12@yahoo.com

Abstract
Timely knowledge of disturbance storm time (*Dst*) index gives us an idea of the severity with which geomagnetic storms may occur, so that possible preventive or remedial measures could be taken. The various techniques for predicting geomagnetic storms are not adequately available for use globally, either since the data required are not available in real time or computing facilities are inadequate. Therefore, the study motivated the current research to improve on the existing models, which is a linear predictive model using the solar wind parameters magnetic field, flow speed and electric field. A total of 74 intense storms during the solar cycle 23 were used. The geomagnetic storms are primarily associated with two classes of drivers, which are the magnetic cloud and the complex ejecta. The correlation coefficients for individual parameters were calculated. The correlation coefficients were highly significant for all the parameters which afforded a predictive model based on multivariance regression analysis. The modeled result shows that the initial and recovery phases of the geomagnetic storms were well predicted, while during the main phase, in some cases, predicted *Dst* is smaller than the measured *Dst*. The difference between the measured and predicted *Dst* suggests that the geomagnetic storm phenomena like pre-storm phenomena could result from some underlying mechanism that is working together with varying degrees of importance and is probably not adequately captured by available solar wind parameters.

Keywords: Disturbance storm time (*Dst*), Geomagnetic **s**torm, Fast solar wind speed, Magnetic cloud, complex ejecta

Introduction

The earth's magnetosphere responds to the ever-changing solar-wind conditions in various ways. Some of the resulting magnetospheric disturbances can be detected at the earth's surface as geomagnetic disturbances due to changes in the large scale electrical current systems flowing in the magnetosphere and ionosphere. A widely used index for quantifying the disturbance level is disturbance storm time (Dst), initially introduced by Sugiura (1964) to measure the ring current magnetic field. This index is defined as the reduction of the horizontal magnetic component at the geomagnetic dipole equator, and has often been used in studies of solar wind-magnetosphere coupling. (akasofu,1981).

The Dst index is intended to measure the symmetric ring current directly. It is a well-known fact that rapid variations of the geomagnetic field can be harmful to technological systems. But the ring current variations are normally not very rapid compared to the substorm effects at higher latitudes. Furthermore, the magnitude of *Dst* variations is smaller than the magnitude of high latitude magnetic disturbances. Why should we make *Dst* forecast? *Dst* approximately measures the strength of the ring current and an enhanced ring current, indicated by a decrease of the *Dst* index, which indicates a major impact on the structure and location of the magnetosphere regions and the boundaries that separate them. On a global scale, the ring current generates a magnetic moment that augments the Earth's magnetic moment as presented on the solar wind. (Sharifi et.al. 2006).

For these reasons, many specific models that characterize the state of the near-Earth space environment are parameterized in Dst. Operational *Dst* forecasts provide us with inputs to such models and give much about current and upcoming space weather conditions. Another reason to make *Dst* forecasts is that some of the most adverse effects of space weather take place during magnetic storms, and the ring-current strength is the basic defining property of a magnetic storm. The *Dst* index can thus be used as a proxy for many types of disturbance that occur during a storm, even though the space weather effects are not directly caused by the ring-current magnetic field variations.

When the interplanetary magnetic field (IMF) reaches the earth with a southward orientation, magnetic reconnection between the earth's magnetic field and IMF will take place. As a result, the earth's magnetic field will be able to connect to the IMF density, so that energetic particles in the solar wind are free to enter the magnetosphere along the magnetic field lines. If the process continues for several hours, the magnetic field, as well as plasma in the magnetosphere, will be strongly distributed by the solar wind and a geomagnetic storm or substorm will be develop (Gonzalez et al. 1994). It is thus evident from the above fact that the flow speed (V), the southward turning of magnetic field (Bz) and Bz duration during magnetic activity play a major role in the magnetic field intensification of the ring current during geomagnetic activities.

Ballatore (2002) points out that there is a saturation effect of fast solar wind on geomagnetic storms (*Dst* not keeping up with larger solar wind speeds). Also, many combinations of interplanetary V and the magnetic field component Bz directed southward have been used as coupling functions for solar wind–magnetosphere interaction, but most of these are particular cases of general expressions of the electric field and the energy transfer at the magnetopause due to large-scale reconnection. In simple terms, the parameter related to geomagnetic *Dst* would be the product VBz. Gonzalez, et al. (2004), Bakare and Chukwuma (2010) has been formulated as *Dst* is assumed to be proportional to the product VBz, thus *Dst* α VBz. This is a key assumption (V is the maximum solar wind speed observed by near-Earth satellites). From the examination of several dozen of magnetic clouds, Gonzalez et al. (1998), Dal Lago, et al. (2001), Bakare and Chukwuma (2010) found that the peak values of the solar wind speed V are related to the total magnetic field intensity B of the magnetic clouds at 1 AU (near Earth), thus V α B.

Geomagnetic Observation Data and Selection of Events

The data used in this study consist of hourly average definite multi-spacecraft interplanetary parameters data of wind flow speed, interplanetary magnetic field Bz component. Hourly values of the low latitude magnetic index Dst were secured from National Space Science Data Centre's

(NSSDCs) OMNIweb service (htt://nssdc.gsfc.nasa.gov/omniweb). Most magnetic clouds were obtained from the wind magnetic field investigation (MFI) (http://lepmfi.gsfc.nasa.gov/mfi/mag_cloud_pub1.html).

It must be noted that solar cycle 23 is the first cycle in which coronal mass ejection (CME) data are available over the whole cycle since the first detection of CMEs in the early 1970s. The availability of simultaneous space and ground-based data covering the Sun-Earth space has made the solar cycle 23 storms one of the best sets of events that could serve as a bench mark to compare storms of future and past cycles (Gopalswamy, 2009). The data for almost the entire solar cycle 23 were studied and analyzed to study the relationship between the low latitude magnetic index Dst and solar wind conditions. A study of 83 intense geomagnetic storms during 1996-2006 has been carried out. The geomagnetic storms are primarily associated with two classes of drivers: the magnetic cloud and complex ejecta.

The corresponding response of the magnetosphere has been quantified by the Dst index. In all the 83 intense geomagnetic storms and due to the paucity of data, 74 intense geomagnetic storms, having $Dst_{min} \leq -100$ nT, have been analysed. The geomagnetic storms developed in the northward IMFs were eliminated. Of the 74 intense geomagnetic storms analysed during the solar cycle 23, the magnetic cloud comprised nearly (50%) of the storms while complex ejecta consisted of 50%. This result agrees with the works of Cane et al. 1997, Burlaga et al. 2001 who found a ratio of 50% on an average between magnetic cloud and complex ejecta. Tables 1 and 2 summarize the details of the interplanetary plasma parameter under consideration.

Model Description

The multiple regression models can be expressed as

$$y = \alpha+\beta_1x_1, \beta_2+x_2, \beta_3+x_3+.............\beta_nx_n+e \quad (1)$$

Where *Y*= the dependent variable, *α* = the intercept parameter β_1, β_2, β_3 = the slope parameters or partial regression coefficients, *e* = the error term and x_1, x_2,x_3= the independent variables

Expand by adding one term for each new independent variable. For illustration purposes, only two independent variables would be used. However, it should be noted that the same approach in principle applies to any number of independent variables. In a symbolic form, the multiple regression equation yields:

$$y = \alpha+\beta_1x_1, \beta_2+x_2, \beta_3+x_3+.............\beta_nx_n+e \quad (2)$$

By minimizing the error term we have,

$$\sum e^2=\sum(y-\alpha-b_1x_1-b_2x_2)^2 \quad (3)$$

$$\frac{d\sum e^2}{da} = -2\sum(y-\alpha-b_1x_1-b_2x_2)=0 \quad (4)$$

$$\frac{d\sum e^2}{db_1} = -2\sum x_1(y-\alpha-b_1x_1-b_2x_2)=0 \quad (5)$$

$$\frac{d\sum e^2}{db_2} = -2\sum x_2(y-\alpha-b_1x_1-b_2x_2)=0 \quad (6)$$

from (4) $\sum Y = na+b_1x_1+b_2x_2$ (7)

from (5) $\sum Yx_1 = \alpha\sum x_1+b_1\sum x_1^2+b_2\sum x_1x_2$ (8)

from (6) $\sum Yx_2 = \alpha\sum x_1+b_1\sum x_1x_2+b_2\sum x_1^2$ (9)

In simple linear regression analysis, there are just two variables one dependent variable (Y) and one independent variable (X). Multivariance Recursion regression analysis has more than one independent variables (x_1, x_2, x_3....x_n), and one dependent variable (y). The strength and the extent to which the independent variables (X_n) explain the variation or multiple regression/correlation coefficient, written as R. when this R is squared, R^2, it tells us the extent to which the independent variable accounts for the variance in the dependent variable. The important output from a multivariance Recursion regression analysis is also noted. There are two kinds: firstly, the estimated squared multiple regression coefficients R^2. As noted, R^2 estimates the amount of variation in the independent variables which is explained by the independent variables. Secondly, the estimated regression weights, otherwise known as the weights, β_n. The weights are attached to each independent variable, $\beta_n X_n$, and tell us the extent or importance of each independent variable in predicting the dependent variable. The R^2 varies between 0 and 1, or 0% to 100%. The higher the value, the more of the variance in the dependent variable can be explained by the independent variables.

For this study, the modeled data comprised ten years of Dst index (1996-2006). The calculated Dst is the sum of several terms.

Dst = Intercept parameter + (partial regression coefficient)(Flow speed) + (partial regression coefficient)(IMF Bz terms) + error terms. I.e. Dst = 34.1959Bz + 3.43577 – 0.120952V.

The technique used and tested for its reliability prediction of geomagnetic indices is called Multivariance Recursion Regression. It is based on the same assumptions and procedures for simple linear regression. The main advantages of multivariance Recursion regressions are that it allows researcher to utilize more of the available information to estimate the dependent analysis

In addition, the contribution of each of the independent variables to the way the regression conducted fits can be determined. Generally, the regression equation performs two functions – predictive and explanatory functions. The predictive function involves the quantitative illustration of analysis with the aim of maximizing the variance in the dependent variables that are accounted for by a given set of independent variables. The explanatory function is an attempt to explain the separate influence of each of the independent variables to establish the importance of the relationship between independent variables and dependent variables.

Predictions of growth and decay of geomagnetic storms using solar wind parameters will continuously be given necessary attention because of its availability of space data covering the Sun-Earth space. Although, it is difficult to compare the different prediction models, the correlation between measured and computed geomagnetic activity indices depends on the type of index, averaging of data, and the statistical properties of the sample used for testing that method.

Predicting Geomagnetic Storms

The geomagnetic storm can be generated under different kinds of solar wind conditions. Two classes of geomagnetic storms have been identified for the present study: Magnetic cloud and complex ejecta. The data used in this study consist of low latitude magnetic index Dst plotted against solar wind multi-spacecraft interplanetary parameters data: wind flow speed V, interplanetary magnetic field Bs components. The correlation coefficient for individual parameters was calculated. It was observed that the correlation coefficient was highly significant for all the parameters hence the data now used, as described in section 3 obtain a predictive model.

Table 3 shows the linear fit correlation relationship between the Dst and B, Dst and Bz, Dst and V, and Dst and VBz, observations during the geomagnetic storms periods. The bolded values represent the more correlated coefficient values for each corresponding set of data. The Dst versus Bz relationship is better represented than the Dstversus B pair for the entire period. While for the Dst versus VBz pair, the observation performs better than the Dst versus V pair.

Table 1: Details of interplanetary magnetic cloud plasma parameters during intense geomagnetic storms

S. No.	Date	Dst, -nT	B, nT	Bz, -nT	V, km s^{-1}	VBz
1	22 Oct 1999	237	35.8	30.7	672	20630.4
2	12 Aug 2000	235	33.6	28.7	671	19257.7
3	24 Nov 2001	221	56.9	27.8	1934	53765.2
4	25 Sep 1998	207	28.7	17.9	839	15018.1
5	17 Sep 2000	201	39.5	23.9	835	19956.5
6	26 Jan 2004	197	25.3	19	1027	19513
7	5 Oct 2000	182	26.3	20.2	578	11675.6
8	22 Sep 1999	173	28.4	15.8	594	9385.2
9	28 Oct 2001	157	18.8	14.5	502	7279
10	8 Nov 1998	149	35.4	19.7	633	12470.1
11	18 Apr 2002	149	30.4	18.1	611	11059.1
12	19 Mar 2001	149	21.5	18.8	490	9212
13	25 Jul 2004	148	23.6	18.8	604	11355.2
14	18 Aug 2003	148	22	15.8	498	7868.4
15	15 Dec 2006	146	17.7	14.5	839	12165.5
16	16 Jun 2003	141	19.5	16.7	625	10437.5
17	12 Feb 2000	133	20.6	16.4	586	9610.4
18	11 Oct 1997	130	13.2	9.7	431	4180.7
19	29 Oct 2000	127	18.8	12	404	4848
20	30 Aug 2004	126	15	14.3	443	6334.9
21	18 Feb 1999	123	27.9	21.8	671	14627.8
22	15 May 1997	115	25.3	23.9	483	11543.7
23	4 Apr 2004	112	17.9	15.1	514	7761.4
24	14 Apr 2006	111	19.8	14.2	540	7668
25	7 Nov 1997	110	18	12.3	468	5756.4
26	19 Oct 1998	110	26.2	16.6	430	7138
27	4 Sep 2002	109	18.6	18.3	461	8436.3
28	23 May 2002	109	38.2	14.1	871	12281.1
29	23 Nov 1997	108	15.7	12.6	581	7320.6
30	21 Apr 1997	107	13.9	8.5	394	3349
31	14 Oct 2000	107	13.6	11.4	442	5038.8
32	23 May 2002	106	38.2	14.1	871	12281.1
33	13 Jun 2005	105	24.2	16.6	508	8432.8
34	12 Jun 2003	105	16.7	12.4	586	7266.4
35	20 May 2005	103	15	9.1	476	4331.6
36	22 Apr 2001	102	15.1	12.8	384	4915.2
37	2 Aug 2002	102	15.7	11.6	540	6264

Note: The peak values of the parameters were used during events intervals

Table 2: Details of interplanetary complex ejecta plasma parameters during intense geomagnetic storms

S. No.	Date	Dst, -nT	B, nT	Bz, -nT	V, km s^{-1}	VBz
1	24 Aug 2005	216	52.2	38.3	720	27576
2	4 May 1998	205	38.9	28.6	833	23823.8
3	21 Oct 2001	187	28.4	15.7	668	10487.6
4	8 Sep 2002	181	19.8	9.5	495	4702.5
5	1 Oct 2002	176	24.8	21.8	421	9177.8
6	30 Jul 1999	173	27.4	15.8	594	9385.2
7	1 Oct 2001	166	23.1	20.9	573	11975.7
8	6 Nov 2002	159	15.1	12.5	609	7612.5
9	9 Nov 2000	159	24.1	12.5	604	7550
10	26 Aug 1998	155	16.1	14.2	801	11374.2
11	22 Jan 2004	149	25.4	14.9	666	9923.4
12	11 Sep 2005	147	18.2	8.5	1059	9001.5
13	29 May 2003	144	28.4	12.7	803	10198.1
14	24 May 2000	142	34.1	19.2	684	13132.8
15	6 Aug 1998	138	21.3	19.3	428	8260.4
16	30 May 2005	138	18.6	16.1	487	7840.7
17	13 Nov 1998	131	20	17.6	407	7163.2
18	31 Aug 2005	131	18.6	15.3	413	6318.9
19	21 Nov 2002	128	32.3	9.3	727	6761.1
20	3 Oct 2002	128	32.2	13.1	713	9340.3
21	8 May 2005	127	16.1	13	804	10452
22	18 Jan 2005	121	20.2	15.5	997	15453.5
23	29 Nov 2000	119	13.9	10.3	558	5747.4
24	7 Oct 2002	115	13.6	8.4	463	3889.2
25	17 Apr 2001	114	23.8	19.6	518	10152.8
26	13 Jan 1999	112	18.7	13.5	421	5683.5
27	11 May 2002	110	18.2	16.5	341	5626.5
28	11 Feb 2004	109	20.8	13.6	444	6038.4
29	18 Apr 2004	109	23.8	19.6	512	10035.2
30	21 Aug 2002	106	9.8	9.2	461	4241.2
31	13 Nov 1999	106	14.7	11.5	482	5543
32	12 Jul 2003	105	14.3	13.2	664	8764.8
33	22 Jan 2005	105	29.5	6.3	943	5940.9
34	17 Aug 2001	105	32.1	18.1	599	10841.9
35	21 Aug 2002	104	9.8	9.1	489	4449.9
36	26 Sep 2001	102	15.9	6.4	671	4294.4
37	28 Jun 1998	101	14.2	13	491	6383

Note: The peak values of the parameters were used during events intervals

Table 3: Correlation relationship between Dst and solar wind plasma parameters during the period 1996 to 2006

Storm date	Dst vs B	Dst vs Bz	Dst vs V	Dst vs VBz
Magnetic cloud	**0.61**	**0.77**	**0.55**	**0.68**
Complex ejecta	**0.58**	**0.60**	0.22	**0.65**
Total no of geomagnetic storms	**0.60**	**0.67**	0.44	**0.67**

Bolded values represent the more correlated coefficient values for each corresponding set of data

Figure 1 shows the plot of both measured and predicted low latitude index *Dst* against time (UT) for the period 12-16 April 2006. From the result beginning from 0:00UT, both measured and predicted value of *Dst* variation show that the storm was weak till 02:00UT on April 14 when the measured Dst value gradually decreases to a minimum value of -111nT at 09:00UT on the same day before recovering. It is observed that the recovery phase takes more than two days. Vieira *et al.* (2001) had classified geomagnetic storms with *Dst* below -100nT as intense geomagnetic storms. The storms main phase development is rapid and the decrease is monotonic. However, the predicted value of Dst shows some variation when it commences decreasing at 22:00UT on April 13 to a minimum value of -76nT at 04:00UT on April 14.

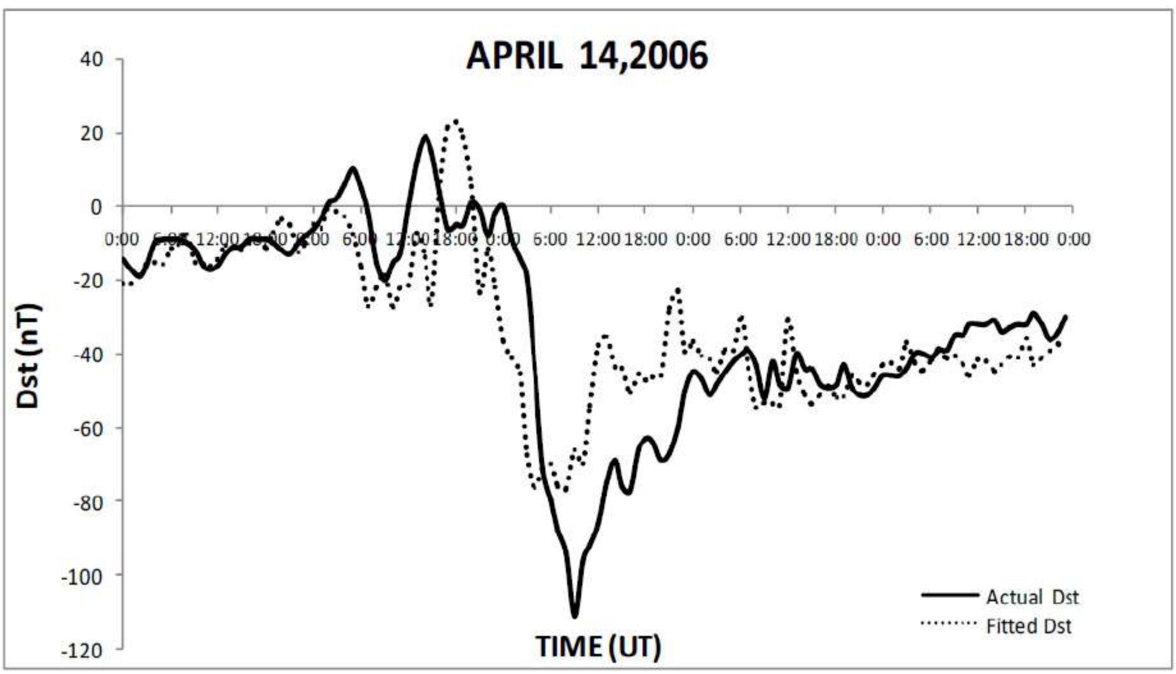

Figure 1:- The *Dst* for the storm of April 12-16, 2006, predicted from the solar wind parameters as the input in the multivariance Recursion regression technique

Figure 2 shows the plot of both measured and predicted low latitude index *Dst* against time (UT) for the period 18-22 November 2003. The results of measured Dst indicate a weak geomagnetic storm on 18-19 November. On 20 November ~10:00UT the Dst experienced a sudden decrease which got to a minimum peak -422nT at 21:00UT on November 20. It was gradually and steeply recovered for the next 24hours. The storm main phase development is rapid and the decrease is monotonic. However, predicted value of *Dst* indicate a weak and moderate geomagnetic storm on 18 and 19 November respectively. Dst show some variation when it commences to decreases at 02:00UT on November 20 to a minimum value of -111nT at 06:00UT. Thereafter, Dst recovered gradually to -5nT at 10:00UT before decreases to a minimum value -312 at 16:00UT on 20 November.

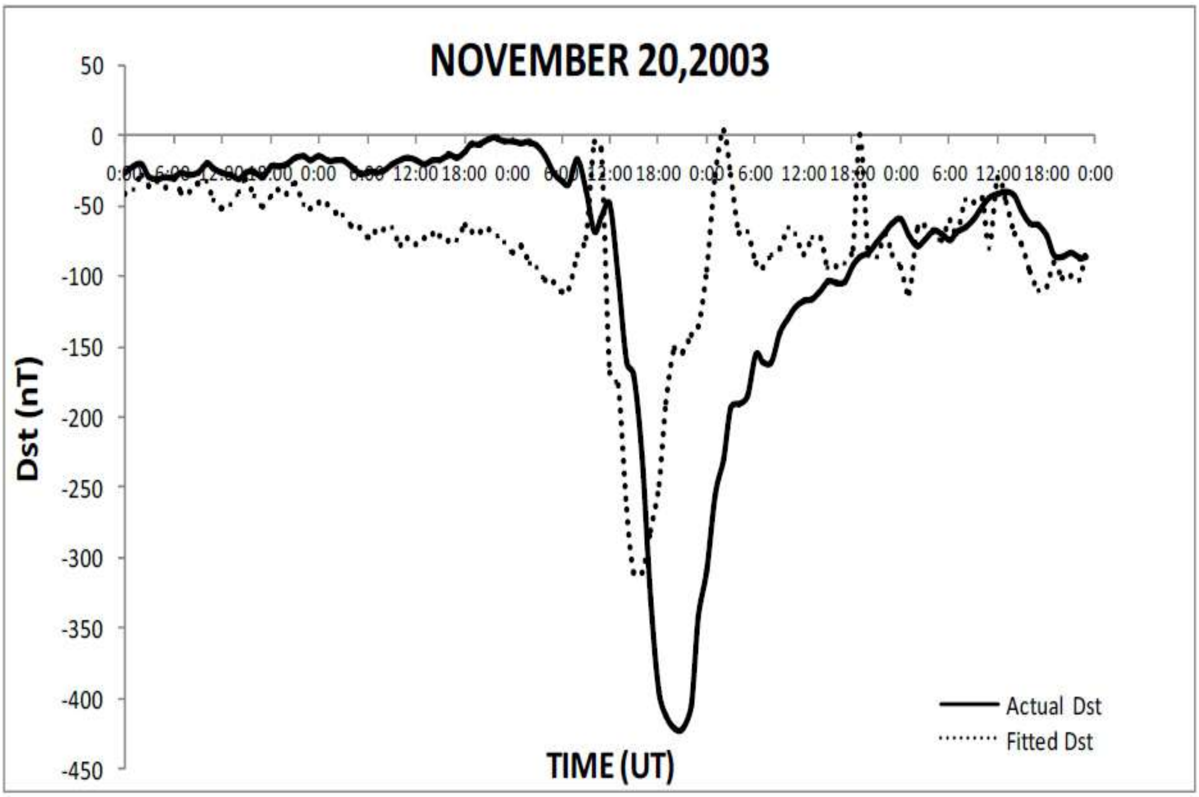

Figure 2:- The *Dst* for the storm of November 18-22, 2003, predicted from the solar wind parameters as the input in the multivariance Recursion regression technique

Figure 3 shows the plot of both measured and predicted low latitude index *Dst* against time (UT) for the period 13-17 May 1997. The measured and predicted Dst plot indicates a weak geomagnetic storm on 13-14 May. On 15 May ~02:00UT the Dst experiences a sudden shock that orientate to the northward direction with peak value of 18nT. Suddenly it decreases sharply to a minimum peak value -115nT at 15:00UT on May 15. It was gradually and steeply recovered through 15-17 May. However, predicted value of *Dst* show some variation when it commences to decreases at 02:00UT on May 15 to a minimum value 0f -91nT at 11:00UT on May 15. Thereafter, Dst recovers rather gradually and steeply recovered through 15-17 May.

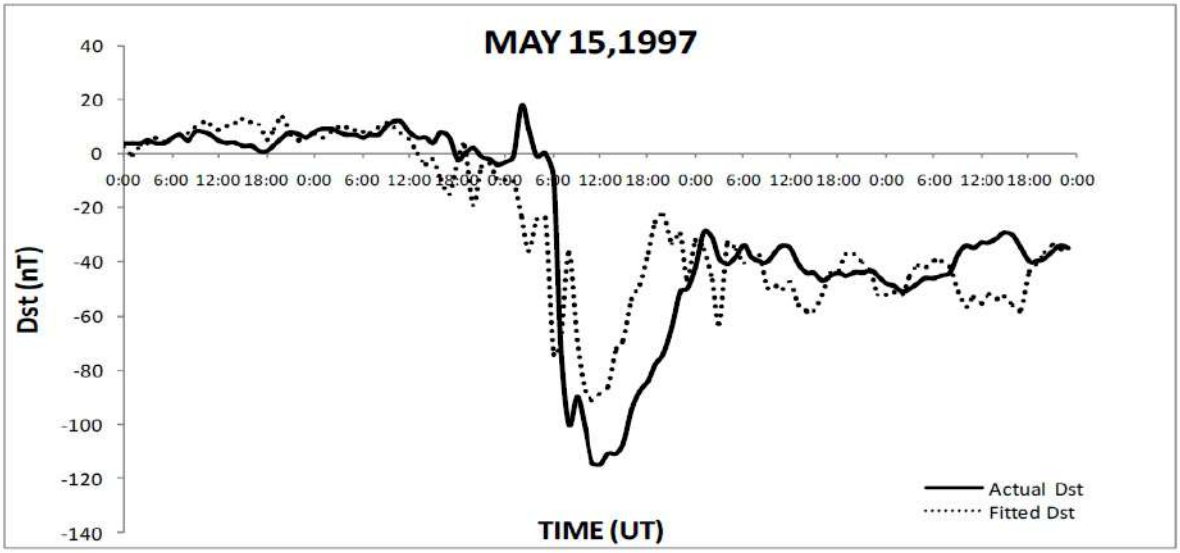

Figure 3:- The *Dst* for the storm of May 15, 1997, predicted from the solar wind parameters as the input in the multivariance Recursion regression technique

Figure 4 also shows the plot of both measured and predicted low latitude index *Dst* against time (UT) for the period 09-13 September, 2005. The measured and predicted Dst plot indicate a weak and moderate geomagnetic storm on 09-10 September, respectively. On 11 September ~02:00UT the Dst experiences a sudden decrease to a minimum value of -147nT at 10:00UT.T It was gradually and steeply recovered through 11-13 September. However, predicted value of *Dst* show some variation when it commences to decreases at 09:00UT on September 11 to a minimum value 0f -96nT at 13:00UT on September 11. Thereafter, Dst recovers rather gradually and steeply recovered through 11-13 September.

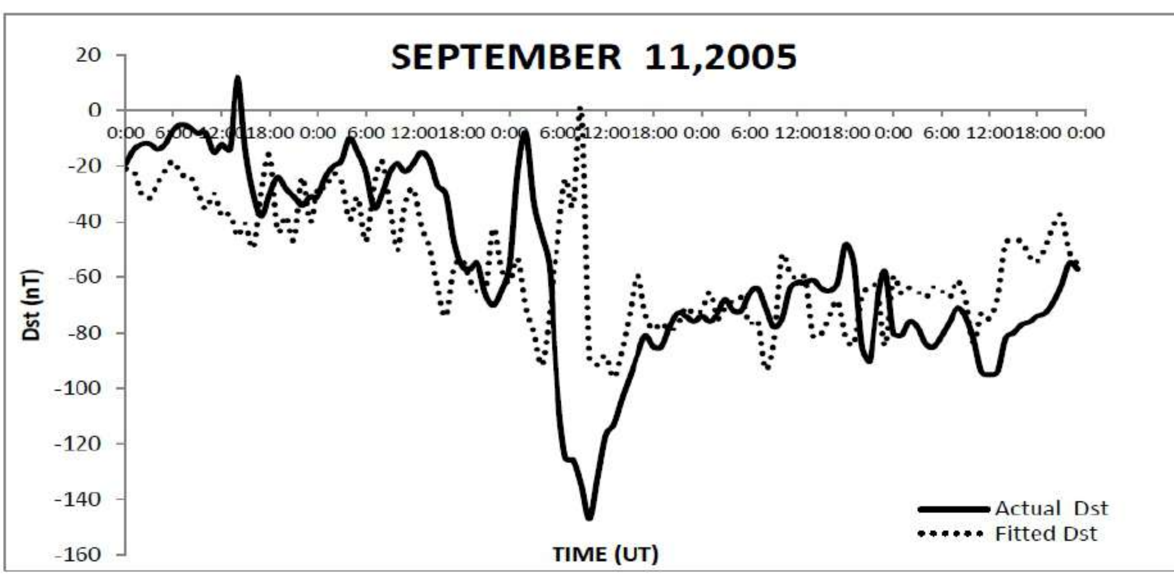

Figure 4:- The *Dst* for the storm of September 11, 2005, predicted from the solar wind parameters as the input in the multivariance Recursion regression technique

Figure 5 shows the plot of both measured and predicted low latitude index *Dst* against time (UT) for the period 29 May-2 June 2001. From the plot beginning from 0:00UT both measured and predicted value of *Dst* variation show that the storm was moderate till 04:00UT on May 29 when the measured Dst value started gradually decreases to a weak storm for the next 48 hours. The storm then decrease to a minimum value of -387nT at 08:00UT on May 31 before started to recovered, and then have a minimum peak of 284nT at 21:00UT on the same day. It is observed that the recovery phase take about two days. However, predicted value of *Dst* show some variation when it commences to decreases to first peak of -189nT at 6:00UT on May 3, 24 hours later it decrease to a minimum value of -209nT at 06:00UT on June 1.

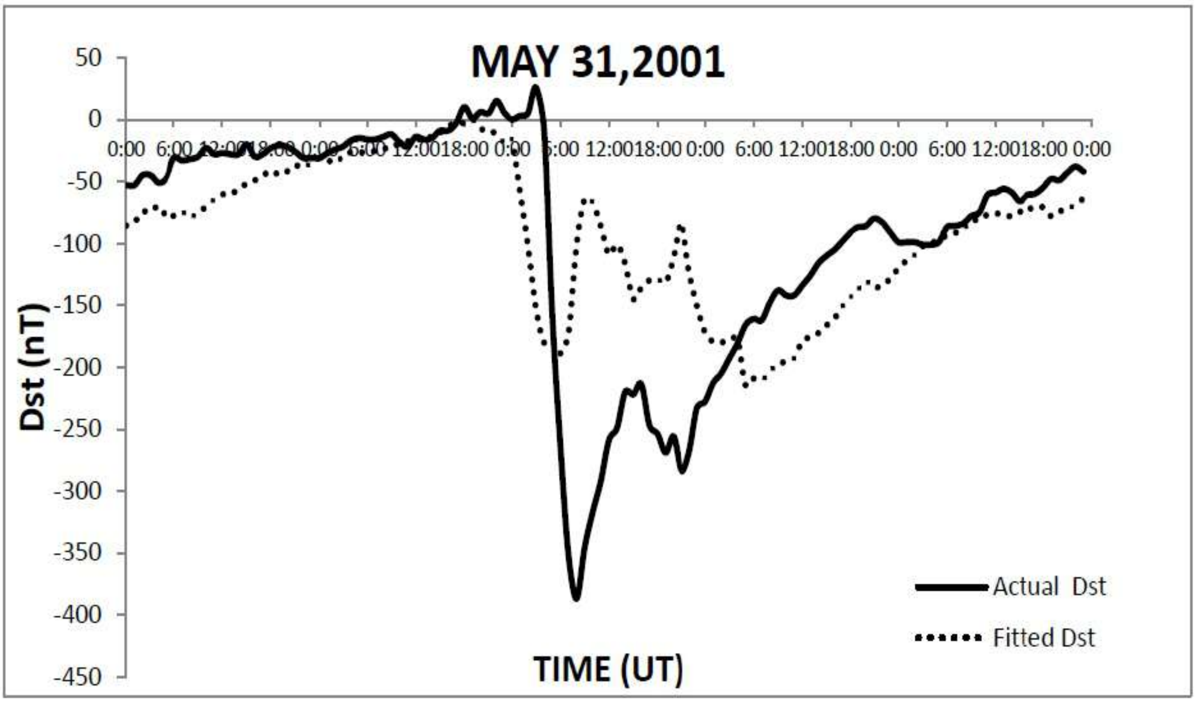

Figure 5:- The *Dst* for the storm of May 31, 2001, predicted from the solar wind parameters as the input in the multivariance Recursion regression technique

The root mean square (RMS) deviation defined by $RMS_{dev} = sqrt\ (Vz_{modelled} - Vz_{observed})\ /\ sqrt\ (n)$ mean error deviation and error values is presented in Table 4. The variance (or the standard deviation) is a measure of the dispersion or scatter of the values of the random variable about the mean. If the values tend to be concentrated near the mean, the variance is small; while the variance is large if the values are distributed far from the mean.

For a given value of x, say x_i there will be a difference between the value y_i and the corresponding value as determined from the curve. i denote this difference by d_i, which is sometimes referred to as a deviation, error, or residual and may be positive, negative or zero. A measure of the goodness of fit of the curve to the set of data is provided by the quantity d_i. If this is small the fit is good, if it is large therefore make the following fit is bad. In spite of this deduction, both the actual Dst and fitted Dst observations revealed a better agreement for the initial and recovery phase than the main phase observation.

Table 3: RMS deviation between the actual Dst and fitted Dst in comparison with modeled observation

Storm date	Total storm period	Initial phase	Main phase	Recovery phase
April 14, 2006	**16.77**	**13.55**	**30.45**	**7.49**
Nov. 20, 2008	**80.42**	**39.27**	**137.27**	**72.17**
May 15, 1997	**18.29**	**6.55**	**36.00**	**12.04**
May 31, 2001	**74.85**	**23.07**	**156.09**	**35.92**
Sept. 11, 2005	**24.85**	**20.12**	**40.22**	**18.16**

Bolded values depicts quantities that shows corresponding better agreement with the set of data.

Discussion

The relationship of Dst index with interplanetary plasma parameters under consideration can be summarized using the plots depicted in Figs 1 - 5. The results reveal some degree of simultaneity as the correlation coefficient for individual parameters was calculated. It was observed that the correlation coefficient was highly significant for all the parameters and that there is no need for classification of geomagnetic storms under any kind of solar wind conditions for modeling purposes. This algorithm for predicting the ground-based *Dst* index is solely from a knowledge of the flow speed and magnetospheric component of the interplanetary magnetic field Bz as shown in equation 1. The algorithm is used to predict the *Dst* signature of some geomagnetic storm in the intervals 1996 and 2006. Figures 1 - 5 show plots for the measured *Dst* and predicted *Dst*. The most striking result is the better performances of predicted *Dst* where we could reproduce 70% of the variable of the *Dst* index (i.e $r^2 \alpha$ 0.70) in the above figures. In order to gain more insight into the physical reason for improved performance of predicted *Dst*, individual geomagnetic storms was studied with all the Figures succeeding the initial and recovery phases of the geomagnetic storms predicting. The predicted onset and strength of the phase is well correlated to the measured *Dst*. The main phases are predicted but the predictions in some cases smaller than the measured main phases.

The main reason for the difference in performance between the measured and predicted *Dst* using different input data sequences sizes was examined. A typical example of this behaviour is in Figs 1 - 5, which shows the measured and predicted Dst indices for a major geomagnetic storm. This indicates two possibilities, namely only a small part of the solar wind history is available to the geomagnetic storms; thus, the predicted main phase in some cases smaller than the measured Dst after only a short time; and or the difference between the measured and predicted Dst appear to suggest that the geomagnetic storm phenomena like pre-storm phenomena could be as a result of some underlying mechanism that is working together with varying degree of importance (Chukwuma, 2010) and is probably not adequately captured by available solar wind parameters.

The results were compared to previous studies using other methods which show that linear filter with solar-wind dynamic pressure and the dawn-to-dusk component of the interplanetary electric field, McPherron et al. (1986) and Fay et al. (1986), were both found that they could account for 70% of the Dst variance. When studying the two filters (i.e.

the P_{dyn}-and the E-filters) separately, McPherron et al. (1986) found that the dynamic pressure filter had a width of only about 10 minutes, while the electric field filter had a very long duration. They drew the conclusion that the characteristic of the electric field filter is due to the long-time constants associated with the decay of the ring current. This is in line with the present finding that the recovery phase predictions depend on the ring current history, and thus the solar wind history.

Another method is to fit an analytical expression to solar-wind and geomagnetic-activity data. An example is Gonzalez, et al.1989 who systematically tested a number of analytical formulas for prediction of the Dst index. They occasionally found correlation coefficients above 0.90 for individual storms, but the average over a more diversed set of storm-time periods was considerably lower. A major advantage of the analytical formulas of Gonzalez et. al. (1989) is that they explicitly reveal the quantitative dependence on the most important solar-wind parameters.

The only method claiming superior correlations to the present study is Goertz et. al.(1993). They used an empirical non-linear model to predict the auroral electrojet index AE and found a correlation coefficient of 0.92. However, the stated correlation was criticized by McPherron and Rostoker (1993) based on an assumed biased selection of test data.

To compare different prediction methods is a difficult task. The correlation between measured and computed geomagnetic-activity indices depends on the type of index, averaging of data, as well as the statistical properties of the sample used for testing the methods.

Conclusion

An investigation into the relationship between Dst index with interplanetary solarwind plasma parameters have been studied from 1996 to 2006 and the following conclusions have been drawn: On average, nearly equal number of magnetic cloud and complex ejecta were found during the intense geomagnetic storms.

The Dst – B relationship results reveal that complex ejecta had overall correlation of 0.71 while magnetic cloud had 0.76, hence their correlation is comparable while complex ejecta had less overall correlation between Dst – Bs than magnetic cloud as the overall correlation is 0.64 and 0.90, respectively during intense geomagnetic storms. The interplanetary magnetic field Bz is an essential interplanetary requirement needed to activate the magnetosphere through reconnection.

A fast solar wind speed and a strong southward component of the magnetic field are particularly effective in producing geomagnetic activity. It is only when the magnetic field of the interplanetary features engulfing the Earth has a strong southward component Bz that a good relationship is obtained between Dst and the product VBz.

Finally, predictions of the growth and decay of geomagnetic storms show that the initial and recovery phases of the storms are well predicted. In contrast, the predicted main phase in some cases is smaller than the measured Dst after only a short time.

References

Akasofu, S.I. (1981): Energy coupling between the solar wind and the magnetosphere, Space Science Reviews,28, 121-190.

Bakare, N.O. and V.U. Chukwuma (2010): Relationship between Dst and solar wind conditions during intense geomagnetic storm Indian J.Radio & Space Phy. 39,150-155.

Ballatore, P., (2002): Effects of fast and slow solar wind on the correlations between interplanetary medium and geomagnetic activity, Journal of Geophysical Research., 107, 1227-1242

Burlaga L F, Skoug R M, Smith C W, Webb, D. F., Zurbuchen, T. H., and Alysha R., (2001): Fast ejecta during the ascending phase of solar cycle 23: ACE observation, 1998-1999, Journal of Geophysical Research, 106, 957- 977.

Cane, H. V., Richardson, I. G., and Wibberenz, G., (1997): Helio 1 and 2 observation of the particle decreases, ejecta, and magnetic clouds, Journal of Geophysical Research, 102, 7075-7086.

Chukwuma V U. (2010): On ionospheric Phenomena during pre-storm and main phase of a varying intense, Acta Geophysicae, 58, 1166-1192.

Dal Lago, A., Gonzalez, W. D., Clua de Gonzalez, A., and Vieira, L. E. A., (2001): Compression of magnetic clouds in interplanetary space and increase in their geo effectiveness, Journal of Atmospheric Solar and Terrestrial Physics 63, 451.

Fay R. A., Garrity, C. R., McPherron, R. L., and Bargatze, L. F., (1986): Prediction filters for the *Dst* index and the polar cap potential. In Kamide Y., and Slavin, J. A., Solar wind-magnetosphere coupling, (pp.111-117), Tokyo, Terra Scientific Publishing Company.

Goertz, C. K., Shan, L. H., and Smith, R. A., (1993): Prediction of geomagnetic activity, Journal of Geophysical Research, 98, 7673-7684.

Gonzalez, W.D., Joselyn, J.A., Kamide, Y., Kroehi, H. W., Rostoker, G., Tsurutani, B.T., and Vasyliunas, V. M., (1994): What is a geomagnetic storm. Journal of Geophysical Research, 99, 5771-5792.

Gonzalez, W. D., Dal Lago, A., Clua de Gonzalez, A. L., Vieira, L. E. A., and Tsurutani, B. T., (2004): Prediction of peak-*Dst* from halo CME/magnetic cloud-speed observations, Journal of Atmospheric Solar and Terrestrial Physics, 66, 161-172

Gonzalez, W. D., Clua de Gonzalez, A. L., Dal Lago, A., Tsurutani, B. J., Arballo, J. K., Lakhina, G. S., Buti, B., and Ho, C.M., (1998): Magnetic cloud field intensities and solar wind velocities, Geophysical. Research Letter, 25, 963- 976

Gonzalez, W. D., Tsurutani, B.T., Gonzalez, A. L. C., Smith, E. J., Tang, F., and Akasofu, S.I., (1989): Solar wind-magnetosphere coupling during intense magnetic storms (1978-1979), Journal of Geophysical Research, 94, 8835-8851.

Gonzalez, W.D, and Tsurutani, B.T., (1987): Criteria of interplanetary parameters causing intense magnetic storms (*Dst*<100nT), Planetary and Space Science 35, 1101- 1109

Gopalswamy, N. (2009): Introduction to special section on large geomagnetic storms. Journal of Geophysical Research, 114, 14026-14030.

Kamide, Y., Baumjohann, W., Daglis, I.A., Gonzalez, W.D., Grande, M., Joselyn, J. A., Mc Pheron, R. L., Philps, J.L., Reeves, E. G. D., Rostoker, G., Sharma, A. S., Singer. H.J., Tsurutani, B. T., and Vasyliunas, V. M., (1998): Current understanding of magnetic storms:storm/substorm relashionship, Journal of Geophysical Research 103, 17,705 -17,728.

McPherron, R. L, and Rostoker, G., (1993): Comment on "Prediction of geomagnetic activity" by Goertz, C. K., Lin-Hua S., and Smith, R. A., Journal of Geophysical Research, 98, 7685-7686.

McPherron, R.L, Baker, D.N., and Bargatze, R.F., (1986): Linear filters as a method of real time prediction of geomagnetic activity. In Kamide, Y. and Slavin, J. A., (eds.), Solar wind-magnetosphere coupling, (pp.85-92), Tokyo, Terra Scientific Publishing.

Sharifi, B., Araabi, N., and Caro L., (2006): Multi-step prediction of *Dst* index using singular spectrum analysis and locally linear neurofuzzy modeling, Earth Planets Space, 58, 331–341.

Sugiura, M. (1964): Hourly values of equatorial; *Dst* for the IGY. Annals International Geophysical Year, 35, (pp.9), New York, Perganon.

Vieira L E, Gonzalez W D, Clua de Gonzalez, A L and Dal Lago A, (2001): A study of magnetic storm development in two or more steps and its association with polarity of magnetic clouds, Journal of Atmospheric Solar and Terrestrial Physics, 63, 457-461.

Wang, C.B., Chao, J. K. and Lin, C.H., (2003): Influence of the solar wind dynamic pressure on the decay and injection of the ring current, Journal of Geophysical Research 108, 1341.